

Characterization of ultrashort terawatt laser pulses by spatially encoded SPIDER technique

© Ya.O. Romanovskii¹, A.V. Mitrofanov^{2,3,4}, P.A. Shcheglov⁴, M.M. Nazarov⁴, D.A. Sidorov-Biryukov^{1,2,4}

¹ Faculty of Physics, M.V. Lomonosov Moscow State University,
119991 Moscow, Russia

² Russian Quantum Center,
121205 Skolkovo Innovation Center, Moscow, Russia

³ Institute on Laser and Information Technologies of the Russian Academy of Sciences — branch of the Federal Scientific Research Center „Crystallography and Photonics“ RAS,
140700 Shatura, Moscow Oblast, Russia

⁴ National Research Center „Kurchatov Institute“,
123182 Moscow, Russia

e-mail: romanovskii.io17@physics.msu.ru

Received December 08, 2022

Revised December 29, 2022

Accepted January 28, 2023

Terawatt laser pulses obtained after temporal compression due to nonlinear spectrum broadening in thin glass plates with subsequent dispersion compensation by chirped mirrors are experimentally characterized by spatially encoded spectral phase interferometry. The proposed method allowed to reconstruct the spectral and temporal phase of obtained 16 fs laser pulses with up to 20 mJ of energy in a single-shot mode with spatial resolution.

Keywords: ultrashort femtosecond pulses, spectrum broadening in transparent dielectrics, spatially encoded spectral phase interferometry.

DOI: 10.61011/EOS.2023.02.55787.9-23

Introduction

Study of physical processes and new phenomena during substance exposure to ultrashort powerful pulses is a challenging task facing modern physics. Powerful laser systems are a unique tool for fundamental research and technology development in physics, astronomy, chemistry and biology [1]. An important development area of multi-terawatt laser systems includes the development of additional external laser pulse compression methods up to the durations at the level of several field oscillation cycles [2,3]. Development of this area is necessary not only in terms of further increase of peak pulse power, but also for those tasks where the use of relativistic intensity few-cycle pulses is essential, for example, such as attosecond pulse generation from a solid target surface [4]. The use of multipetawatt laser emission compression mechanisms to achieve subexawatt [5] and exawatt [6,7] powers will allow to reach ultrarelativistic conditions of interaction with a substance. Today, one of the most promising approaches for the use in multi-terawatt laser systems is the method based on powerful pulse spectrum broadening in thin glasses with further phase compensation by chirped mirrors [2,3,6,8–10]. Joule energy level pulse (peak power about 100 TW) compression is reported from 24 fs to 13 fs [8] and from 23 fs to 9.7 fs [9] with preliminary spatial beam mode cleaning using a dedicated spatial filter. This method of laser pulse time compression is highly sensitive to intensity distribution over

the beam cross-section and intensity fluctuation from pulse to pulse, therefore it is important to control the duration and spectral phase within one laser pulse with spatial resolution.

The paper contains experimental results of characterization of laser pulses with peak power 1 TW achieved by means of temporal compression with nonlinear spectrum broadening in thin glasses with further dispersion compensation by chirped mirrors. For temporal characterization of pulses, we have assembled SEA-F-SPIDER setup [11]. Laser pulses at central wavelength 800 nm with initial duration 27 fs were compressed to 16 fs and were characterized in a single-shot mode with beam cross-section resolution.

Experimental part

Ti:Sapphire laser system [12,13] with pulse duration 27 fs, energies 10–20 mJ and beam diameter about 65 mm was used in our experiments (Fig. 1, a). Laser radiation was focused by a 250 cm focal length spherical mirror in a vacuum system consisting of two vacuum chambers connected with an extended pipe with pressure lower than 10^{-5} mbar. At this residual gas pressure, no nonlinear pulse phase distortion in the beam focus was observed. The pipe contained two thin glass plates (1 mm BK7): the first was placed at 110 cm upstream of the focus, and the second at 75 cm downstream of the focus. The distance was selected to avoid optical breakdown and considerable

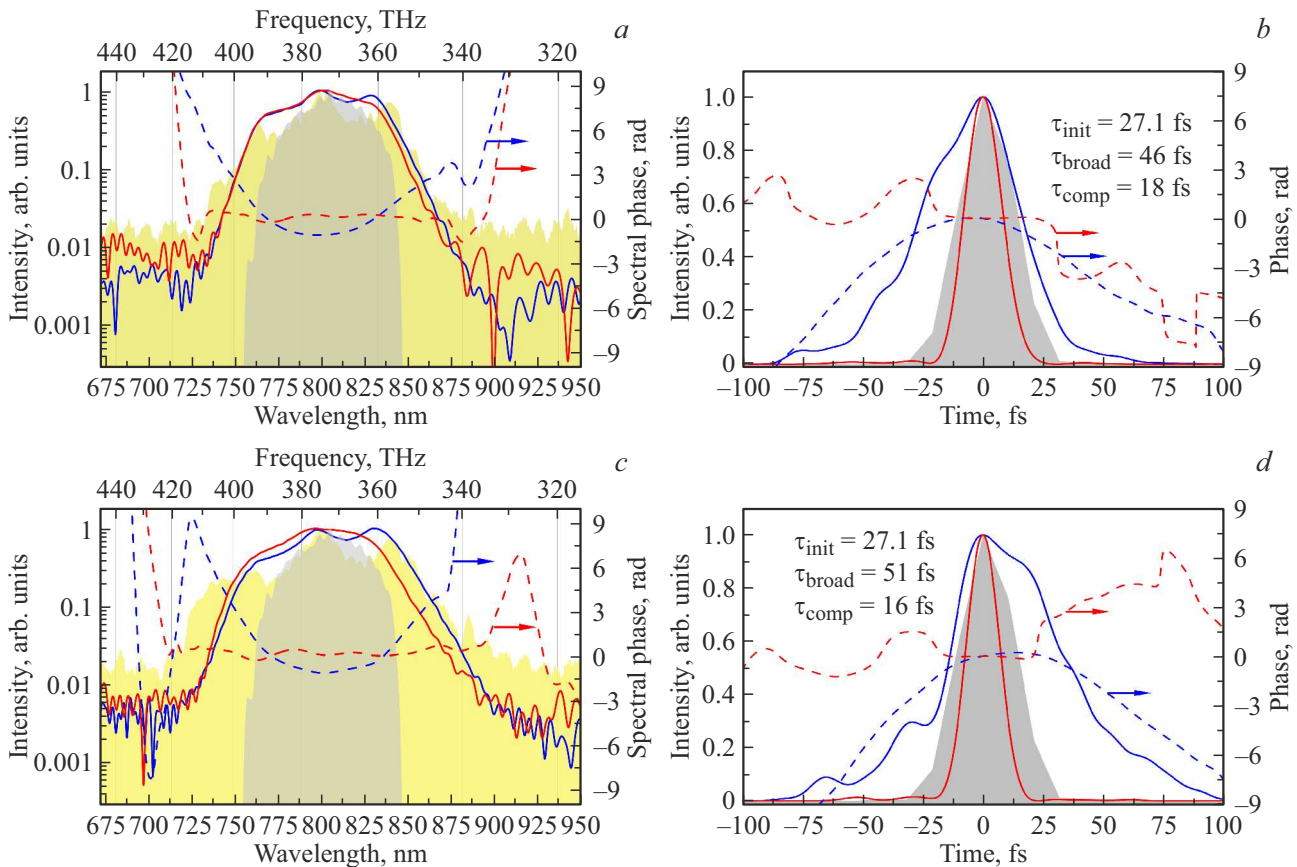


Figure 2. Spectral and temporal intensities and phase. 10 mJ — pulse (a) and (b), 20 mJ pulse — (c) and (d). Grey (background) — spectrum and temporal intensity of the initial pulse (measured using Wizzler). Yellow (background) — broadened spectrum (smoothed with a moving average by 15 points, measured using OceanOptics spectrometer) of the pulse after passing the glass plates. Blue solid line and blue dashed line are, respectively, the pulse intensity and phase with a broadened spectrum without chirp compensation (obtained from SPIDER), red solid and dashed lines are the compressed pulse intensity and phase with broadened spectrum after chirp compensation (obtained from SPIDER).

and having a flat spectral phase. In this case, the influence of W1 quartz exit window was compensated by additional pair of chirped mirrors not shown in the diagram.

To characterize the phase and pulse duration after compression by chirped mirrors we have designed and assembled a system to enable temporal profile characterization of the pulse with spatial resolution along one beam coordinate based on spatially encoded arrangement spectral phase interferometry for direct electric field reconstruction (SEA-F-SPIDER) [11]. It should be noted that the selected technique does not introduce any test pulse distortions, because only reflective optics is directly used in the system for pulse characterization, which is especially important when few-cycle pulses are used. Moreover, reconstruction of the spectral and temporal phases was based on the data acquired during one laser pulse, which allowed to avoid the averaging errors associated with laser emission intensity fluctuations. The basic idea of spectral shear interferometry constitutes the interference recording between a pair of pulses spectrally shifted

against each other. For this, two copies of the test pulse are created using nonlinear frequency interaction with the pair of ancillae pulses. Copies spectrally shifted against each other at Ω interfere at the spectrometer entrance slit. The interference fringe density is determined by a spatial angle between the test pulse copies in SEA-F-SPIDER. Ancillae quasi-monochromatic pulses are produced by passing a part of the measured signal through narrow-band interference filters. Spectral shift Ω is achieved by rotating one filter relative to the other. The resulting interference pattern with spectral resolution along one axis gives a two-dimensional image recorded by CCD-camera.

Figure 1, b shows the diagram of assembled SEA-F-SPIDER system. To characterize the phase of the test pulse, a part of the pulse is reflected from beam splitter BS1, then reflected from the wedge to align the arms by energy and forwarded into the nonlinear crystal. The pulse part that has passed BS1 goes to BS2 and is divided into two pulses with approximately equal energies. These two beams pass narrow-band spectral filters SF1, Edmund

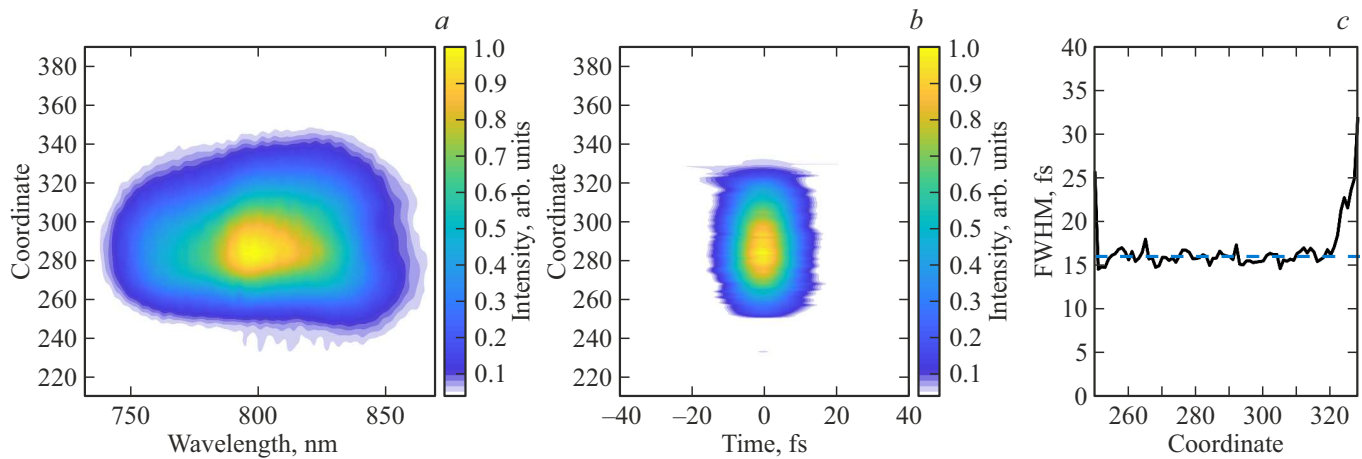


Figure 3. 20 mJ pulse. (a) spectral intensity profile obtained from SPIDER interference pattern, (b) spatiotemporal pulse structure, (c) pulse FWHM along the spatial axis — black line, blue line — 16 fs, corresponding FWHM along the coordinate with maximum intensity.

Optics: 785 nm (FWHM 2.98 nm); SF2, 810 nm (FWHM 3 nm) for formation of a pair of ancillae beams. Change of installation angle SF2 defines the amount of spectral shift Ω . Spectral shift is selected in such a way that it constitutes $1/10$ – $1/20$ from the pulse spectrum width, because the shift shall not be so large that the phase sampling interval could exceed the Nyquist limit and at the same time shall not be so small that the spectral phase difference could not be distinguished by the spectrometer [16]. After the crystal, two frequency shifted copies go in different directions and separated from the second harmonics of the test and ancillae pulses using the mask and then focused by the 10 cm focal length spherical mirror (SM) at the spectrometer entrance with size magnification. The distance between the spectrometer entrance and SM was 135 cm. The collinear test beam and two ancillae beams are focused by the parabolic mirror (focal distance 10 cm) in the BBO nonlinear crystal (thickness $10\ \mu\text{m}$, I type phase matching) for sum-frequency generation of two copies of the test pulse. As 2D-spectrometer Solar SDH-IV was used. It had a Czerny–Turner scheme and Thorlabs BC106-VIS camera (12 bit, workspace 1360×640 pixels) instead of the original linear CCD-matrix. 2D-spectrometer was calibrated by wavelength using individual comparative measurements by Ocean Optics spectrometer. Data from camera is recorded by a computer and processed by Matlab program based on SPIDER [16] phase reconstruction algorithm taking into account the spatial resolution along one of the axes.

Experimental results

Measurements for spectral broadening in dielectric were carried out for pulses with energies 10 mJ and 20 mJ. The initial pulse duration was 27 fs, spectrum width was 76 nm (hereinafter the spectrum width is given at level e^{-2}).

After passing the pair of 1 mm BK7 plates, 10 mJ pulse spectrum broadened to 98 nm (45.6 THz). Logarithmic spectrum and reconstructed spectral phase curve is shown in Figure 2, a. Temporal profile and phase are shown in Figure 2, b. Pulse duration after spectrum broadening without chirp compensation was equal to 46 fs, and after five reflections from chirped mirrors (in total $-270\ \text{fs}^2$), the compressed pulse duration is 18 fs. Due to self-phase modulation, spectrum width of 20 mJ, pulses was increased up to 113 nm (52.5 THz). The durations of broadened and compressed pulses were 51 fs and 16 fs, respectively (Figure 2, c, d). A good correlation of spectrum widths restored from SEA-F-SPIDER technique and directly measured with Ocean Optics spectrometer is obtained at these energies. Moreover, the number of chirped mirrors bounces was selected to fit an almost flat phase and then compensate the chirp induced by self-phase modulation to finally compress the pulse by a factor of 1.7 at these energies.

The used technique allows ones to acquire all laser pulse properties along the spatial axis from the recorded interference patterns. For interference pattern processing, 2D-Fourier transform is used with its result shown in Figure 1, b: the pattern contains one central peak (DC) and two symmetrical (AC) peaks. AC-peaks contain the spectral phase data [11,16], and the central peak contains the spectral intensity data. By means of DC-peak filtration and inverse 2D-Fourier transform, we can obtain the spectral intensity profile for the test pulse. Figure 3, a shows software-reconstructed spectral intensity profile of the compressed pulse for all beam cross-sections with initial energy 20 mJ, Figure 3, b shows spatio-temporal pulse structure. Measurements along the spatial axis of the beam have shown the uniform manner of spectrum broadening and similar compressed pulse duration (Figure 3, c). It is shown that almost on entire transverse axis of the beam, its duration is maintained at 16 fs that corresponds to the pulse duration in the cross-section with maximum intensity.

Conclusion

Thus, a full characterization technique was demonstrated for laser pulses after temporal compression by chirped mirrors with nonlinear broadening of the terawatt emission spectrum in thin dielectric plates. Laser pulses were characterized using SEA-F-SPIDER technique allowing to reconstruct the phase and ultrashort pulse duration along one spatial axis. Laser pulses with initial duration 27 fs and energy up to 20 mJ were spectrally broadened in two glass plates up to 113 nm at level e^{-2} , which allowed to compress them up to 16 fs.

Acknowledgments

The authors would like to express sincere gratitude to professor A.M. Zheltikov, Head of the Laboratory of Photonics and Nonlinear Spectroscopy, under whose supervision the study was carried out.

Funding

The study was partially supported by Russian Science Foundation (grant № 22-22-00964). Education of Ya.O. Romanovsky was supported by Theoretical Physics and Mathematics Advancement Foundation „BASIS“.

Conflict of interest

The authors declare that they have no conflict of interest.

References

- [1] A.M. Zheltikov. *Sverkhkorotkie impulsy i metody nelineinoi optiki* (Fizmatlit, 2006) (in Russian).
- [2] E.A. Khazanov. *Quantum Elect.*, **52** (3), 208 (2022). DOI: 10.1070/QEL18001
- [3] T. Nagy, P. Simon, L. Veisz. *Advances in Physics: X*, **6** (1), 1845795 (2021). DOI: 10.1080/23746149.2020.1845795
- [4] O. Jahn, V.E. Leshchenko, P. Tzallas, A. Kessel, M. Krüger, A. Münzer, S.A. Trushin, G.D. Tsakiris, S. Kahaly, D. Kormin, L. Veisz, V. Pervak, F. Krausz, Z. Major, S. Karsch. *Optica*, **6**, 280–287 (2019). DOI: 10.1364/OPTICA.6.000280
- [5] A.A. Voronin, A. M. Zheltikov, T. Ditmire, B. Rus, G. Korn. *Opt. Commun.*, **291**, 299–303 (2013). DOI: 10.1016/j.optcom.2012.10.057
- [6] G. Mourou, S. Mironov, E. Khazanov, A. Sergeev. *The European Phys. J. Special Topics*, **223** (6), 1181–1188 (2014). DOI: 10.1140/epjst/e2014-02171-5
- [7] A.A. Voronin, A.M. Zheltikov. *UFN*, **186** (9), 957–966 (2016) (in Russian). DOI: 10.3367/UFNe.2016.02.037700
- [8] S.Yu. Mironov, S. Fourmaux, P. Lassonde, V.N. Ginzburg, S. Payeur, J.-C. Kieffer, E.A. Khazanov, G. Mourou. *Appl. Phys. Lett.*, **116**, 241101 (2020). DOI: 10.1063/5.0008544
- [9] J.I. Kim, Y.G. Kim, J.M. Yang, J.W. Yoon, J.H. Sung, S.K. Lee, C.H. Nam. *Optics Express*, **30** (6), 8734–8741 (2022). DOI: 10.1364/OE.452224
- [10] M. Stanfield, N.F. Beier, S. Hakimi, H. Allison, D. Farinella, A. E. Hussein, T. Tajima, F. Dollar. *Opt. Express*, **29**, 9123–9136 (2021). DOI: 10.1364/OE.417404
- [11] T. Witting, F. Frank, C.A. Arrell, W.A. Okell, J.P. Marangos, J.W. Tisch. *Opt. Lett.*, **36** (9), 1680–1682 (2011). DOI: 10.1364/OL.36.001680
- [12] M.M. Nazarov, A.V. Mitrofanov, D.A. Sidorov-Biryukov, M.V. Chaschin, P.A. Shcheglov, A.M. Zheltikov, V.Y. Panchenko. *J. Infrared, Millimeter, Terahertz Waves*, **41** (9), 1069–1081 (2020). DOI: 10.1007/s10762-020-00689-z
- [13] M.V. Kovalchuk, M.M. Borisov, A.A. Garmatina, V.M. Gordienko, A.M. Zheltikov, V.V. Kvardakov, V.N. Korchuganov, I.A. Likhachev, E.I. Mareev, A.V. Mitrofanov, M.M. Nazarov, E.M. Pashaev, F.V. Potemkin, Ya.O. Romanovskii, E.B. Rudneva, D.A. Sidorov-Biryukov, I.A. Subbotin, M.V. Chashchin, P.A. Shcheglov, V.Ya. Panchenko. *Crystallography Rep.*, **67**, 717–728 (2022). DOI: 10.1134/S106377452205008X.
- [14] FASTLITE [Electronic resource]. URL: <https://fastlite.com/produits/wizzler-ultrafast-pulse-measurement/>
- [15] T. Oksenhendler. arXiv:1204.4949 (2012). DOI: 10.48550/arXiv.1204.4949
- [16] C. Iaconis, I.A. Walmsley. *IEEE J. Quantum Electronics*, **35** (4), 501–509 (1999). DOI: 10.1109/3.753654

Translated by E.Ilyinskaya